Hindawi
Journal of Environmental and Public Health
Volume 2023, Article ID 5663261, 14 pages
https://doi.org/10.1155/2023/5663261

Research Article

Optimization and Modeling of Cr (VI) Removal from Tannery Wastewater onto Activated Carbon Prepared from Coffee Husk and Sulfuric Acid (H_2SO_4) as Activating Agent by Using Central Composite Design (CCD)

Amibo Temesgen Abeto,[1] **Bayan Surafel Mustafa**,[1] **Bayu Abreham Bekele**,[1] **and Kabeta Worku Firomsa**[2,3]

[1]*School of Chemical Engineering, Jimma Institute of Technology, Jimma University, Po.Box 378, Jimma, Ethiopia*
[2]*Faculty of Civil and Environmental Engineering, Gdańsk University of Technology, Gdańsk, Poland*
[3]*Faculty of Civil and Environmental Engineering, Jimma Institute of Technology, Jimma University, Po.Box 378, Jimma, Ethiopia*

Correspondence should be addressed to Amibo Temesgen Abeto; temesgen.abeto@ju.edu.et

Received 23 March 2022; Revised 4 October 2022; Accepted 8 October 2022; Published 30 January 2023

Academic Editor: Rahil Changotra

The primary goal of this research is to lower the hexavalent chromium (Cr (VI)) concentration that has occurred from the growth of the tannery industry. As a result, the potential for heavy metal concentration is increasing day by day. Industrial effluent containing Cr (VI) contributes significantly to water pollution. Chromium hexavalent ion (Cr (VI)) in wastewater is extremely hazardous to the environment. It is critical to address such a condition using activated carbon derived from biomass. Adsorption is one of the most successful methods for removing hexavalent chromium from wastewater. Treated wastewater has no substantial environmental contamination consequences. The ash content, moisture content, volatile matter content, and fixed carbon content of wet coffee husk were 3.51, 10.85, 68.33, and 17.31, respectively. The physicochemical properties of coffee husk-based activated carbon (CHBAC) obtained during experimentation were pH, porosity, the yield of CHBAC, bulk density, point of zero charges, and specific surface area of 5.2, 58.4 percent, 60.1 percent, 0.71 g/mL, 4.19, and 1396 m^2/g, respectively, indicating that CHBAC has a higher capacity as an adsorbent medium. For optimization purposes, the parameters ranged from pH (0.3–3.7), dose (2.3–5.7) *g*, and contact time (0.3–3.7) hr. The quadratic models were chosen for optimization, and the *p* value for the model was significant since it was less than 0.05, but the lack of fit model was inconsequential because it was more than 0.05. The optimum adsorption obtained with numerical optimization of Cr (VI) was 97.65 percent. This was obtained at a pH of 1.926, a dose of 4.209 g/L, and a contact time of 2.101 hours. This result was observed at a pH of 1.93, a dosage of 4.2 g/L, and a contact duration of 2.1 hours. The desirability obtained during numerical optimization was 1. Coffee husk-based activated carbon has a bigger surface area, and it has a stronger ability to absorb hexavalent chromium from tannery wastewater effluents.

1. Introduction

Nowadays, wastewater creation has grown due to fast population expansion, excessive water use, and increasing industrialization, contributing to environmental damage. Water used for various reasons, such as housekeeping, washing of various equipment, and machinery in various enterprises, is discharged into the environment without previous treatment. The discharge of wastewater without treatment causes major environmental contamination, affecting living things such as humans, animals living in the environment, and aquatic ecosystems [1].

Growing industrialization increases water absorption and consumption within the environment, yet this consumed water is discharged as waste after use. This industrial wastewater is dumped straight into freshwater without

treatment. The dumped wastewater contains a variety of contaminants [2, 3]. Various operations such as scoring, sizing, mercerizing, printing, coloring, and finishing are carried out in textile factories. The textile industries and tannery industries' operations consume pure water and then emit wastewater. Textile industries' effluents consume approximately 8000 chemical compounds to prepare 400 billion m^2 of fabric cloth each year around the world [4]. Similarly, tannery companies may use water for the pretreatment of skins and hides, as well as consume health-hazardous chemicals at high costs, use rudimentary chemical management methods, and discharge such chemicals into wastewater created by the firm. Chromium is a heavy metal even at low concentrations. It induces toxicity, allergenicity, and carcinogenicity, and occasionally it can block the action of sensitive enzymes [5, 6].

In some industries, various technologies have been used to remediate wastewater discharged from various sectors such as textiles, tannery, and other wastewater-generating businesses. The three main wastewater treatment methods are biological, chemical, and physical [7]. The phenomenon of adsorption has several applications, the most important of which are listed here: removal of heavy metals from solutions; gas masks; production of high vacuum; humidity control; heterogeneous catalysis; removal of coloring matter from solutions; in curing diseases; separation of inert gases; and adsorption indicators. This study focuses on removing coloring matter from solutions and removing heavy metals from solutions [8–11]. Removal of coloring matter and heavy metals from solutions entails preparing Biochar, charcoal, or activated carbon from plant and animal wastes and then utilizing this adsorbent to remove color, odors, turbidity, COD, BOD, heavy metals, and other compounds from the impure solution. There are several ways of physical treatment, such as filtration and sedimentation, which separate contaminants from wastewater without any chemical change or reaction [12]. Biological wastewater treatment primarily employs microbes such as bacteria and protozoa to clean water; in this case, microbes break down large organic waste found in water and convert it to simple compounds via aerobic and anaerobic digestion. This process increases biological oxygen demand (BOD) and chemical oxygen demand (COD) [13]. The chemical technique of wastewater treatment employs chemical reactants to break down contaminants in wastewater [14, 15].

Since the primary heavy metals detected in wastewater include Cr (III), Cr (VI), Zn (II), Pb(IV), and others, the levels of heavy metal concentration have been increasing day by day in many studies. This continuous growth of heavy metals causes significant health and environmental problems [16–18]. Hexavalent chromium can cause major health problems such as liver and kidney illness, diarrhea, nosebleeds, dermatitis, mouth ulcers, cancer, and a decrease in the number of white blood cells, reducing the immune system's ability to resist disease. According to several studies done in 2015, over 16 million people were harmed due to Cr (VI) heavy metal pollution [19]. Several treatment procedures were used to lower the content of Cr (IV) in tannery effluent to address this issue. The most generally utilized strategy for reducing Cr (VI)-containing wastewater is absorption. Agro-industrial by-products are the most often utilized raw materials [20, 21].

Ethiopia is the fifth most coffee producing country globally. This activity results in a large volume of coffee husk creation throughout the year. As a result, the coffee husk is readily available, affordable, and easy to trash and dispose of in the environment, contributing to environmental contamination [22]. In this study, coffee husk-based activated carbon (CHBAC) activated with sulfuric acid was used to reduce the amount of hexavalent chromium in tannery effluent and optimize Cr (VI) adsorption. The adsorption technique is a common way of minimizing the number of contaminants that enter water bodies, and researchers are working on the production of activated carbons from inexpensive sources to replace pricey commercial activated carbons. Activated carbons produced from biomass are characterized by low-volume pores that increase the surface area available for adsorption or chemical reactions. In addition to this, activated carbon exhibited the following properties: a high degree of microporosity, the surface area depending on the type of raw material, and the carbonization process. In this study, the activated carbon produced was chemically treated [3, 23, 24]. Determine the effect of process variables on hexavalent chromium adsorption, such as pH, contact time, and activated carbon dosage. In this investigation, the pH varied from 0.3 to 3.7, the contact time varied from 0.3 to 3.7 hours, and the dose of CHBAC varied from 2.3 to 5.7 g/L. The CCD creates a total of 20 experimental factorial points (8 points), axial points (6 points), and center points based on this (6 points). In this study, coffee husk-based activated carbon was applied directly to industrial wastewater and optimization was performed. Fourier-transform infrared spectroscopy (FTIR), X-ray diffraction (XRD), and Brunauer-Emmett-Teller (BET) were used to characterize the CHBAC, and the adsorption efficiency (%) and adsorption capacity (mg/g) of CHBAC were determined during the removal of hexavalent chromium from tannery effluent.

2. Materials and Methods

2.1. Materials. Sulfuric acids (H_2SO_4) with a concentration of 98.3 percent, hydrochloric acid (HCl) with a concentration of 38 percent, and other chemicals with varying grades were bought from Sigma-Aldrich plc (the United States) and utilized without purification. Tannery wastewater was obtained straight from the Koka tannery (Ethiopia) facility and released from the factory effluents. The concentration of Cr (VI) was then measured using a UV-spectrophotometer (Make and Model: PerkinElmer Lambda 25, USA). Finally, the pH of the wastewater was tested using a pH meter (model number pH-9202, China). FTIR (PerkinElmer spectrum two, wavenumber range 8300–350 cm^{-1}, USA), XRD (Drawell XRD 7000, China)

2.2. Methods. Prior to the manufacture of activated carbon, the raw material was chosen based on its carbon content. As

a result, the coffee husk was chosen for activated carbon preparation. The coffee husk is then processed and crushed before the ashing process. The activated carbon in this study was made from coffee husks utilizing chemical activation methods. This type of chemical activation aids in increasing the surface area of activated carbon.

2.3. Activated Carbon Preparation. The major raw material, coffee husk, was brought to the College of Material Science and Engineering from a wet coffee processing facility in Jimma City, Oromia, Ethiopia, for further processing. Then, distilled water is filtered using a reverse osmosis technique (model number: PURE RO 130) to decrease the ions in the tap water, resulting in a conductivity of fewer than 0.6 μmhos/cm. Wet coffee husk is dried in the sun for three days before being rinsed with distilled water to remove dust and other filth that has adhered to it. It is then placed in an oven (model number: DHG-9203A, Germany) at 105°C for 24 hours. As a result, the oven-dried coffee husk was ground in a laboratory scale ball mill to decrease the size, which was then submitted to mesh analysis, and the size kept between 0.25 mm and 0.1 mm was used for subsequent studies. Following that, an evenly sized coffee husk is impregnated with 3 percent sulfuric acid as a chemically activating agent. The w/v ratio of CH to H_2SO_4 is 1 : 3. Finally, the sample was submitted to a muffle furnace (model number: L31M, Germany). The temperature was adjusted to 850°C. The ashing process was continued for 2 hours before being removed when the muffle furnace was cooled.

2.4. Characterization of the Coffee Husk (CH). The coffee husk ash content, volatile matter, and moisture content were examined with certain adjustments by Amibo et al. [14]. This helps to establish the fixed carbon content found in Coffee Arabica. The moisture content and volatile matter of the coffee husk were determined using a digital oven (model: DHG-9203A). The ash content of the coffee husk was evaluated using a muffle furnace (model number: L31M, Germany). As a result, the fixed carbon content is calculated by subtracting the percent of ash, volatile matter, and moisture content from the hundred existing bases.

2.5. Characterization of Coffee Husk Activated Carbon (CHBAC). The activated carbons made from coffee husk before and after adsorption were then analyzed using a Fourier transmission infrared spectrophotometer (FTIR) analysis, X-ray diffraction (XRD) analysis, and Brunauer-Emmett-Teller (BET) for CHBAC surface area analysis. The functional group identified in CHAC impregnated with sulfuric acid as an activating agent was determined via FTIR analysis. The existence of a crystallinity index in activated carbon derived from the coffee husk and after Cr (VI) adsorption was determined using XRD analysis. BET to estimate the diameter of the activated carbon particle size. The porosity of CHBAC and the surface area of activated carbon were determined [23].

2.6. CHBAC Point of Zero Charge Determination. Three methods were used to determine the points of zero charge for activated charcoal, granite sand, lakhra coal, and ground corn cob materials: the first method is the pH drift method, which measures pH where the adsorbent behaves as a neutral specie; the second method is potentiometric titration, which measures the adsorption of H^+ and OH^- on surfaces in solutions of varying ionic strengths; and the third method is direct assessment of the surface charge via nonspecific ion adsorption. From those methods, the first method was employed for this study [25].

2.7. Experimental Design for Optimization of Cr (VI) Adsorption. The central composite design was used for Cr (VI) adsorption optimization, so software was used (Design of Expert-V.11) [26]. The three primary variables employed for optimization were adsorbed dose, pH, and contact time. These variables were chosen based on existing research that has shown that they have a considerable impact on the adsorption process. A total of 20 experimental points were developed by applying response surface methods, especially central composite design. These experiments were divided into three major parts: 8 factorial points, 6 axial points, and 6 central points. The total number of experiments was represented by the following equation and the predicted value from the central composite design was determined by equation (2).

$$T = 2^m + 2m + m_c, \tag{1}$$

where T stands for the total number of experiments, m stands for the number of the independent variable, and m_c stands for center points.

$$R = b_o + \sum_{i=1}^{m} b_i x_i + \sum_{i=1}^{m} b_{ii} x_i^2 + \sum_{i=1}^{m} \sum_{j=i+1}^{n} b_{ij} x_{ij}, \tag{2}$$

where R stands for predicted values from central composite design, m stands for independent variables, b_i, b_{ii}, and b_{ij} represent the linear and quadratic coefficients of interaction effects.

3. Result and Discussion

3.1. Proximate Analysis of Coffee Husk. Proximate analysis for CH was carried out to determine the fixed carbon content, ash content, moisture content, and volatile matter content using various standard methods, as shown in Table 1. The moisture content of the coffee husk was 10.85 percent, which is comparable to the moisture content of the coffee husk previously reported and presented by Amibo et al. [14] for the study. The result was 10–11 percent. Menya et al. [29] for the study from dry-based rice husk, the moisture content was found to be 6.0 to 7.7 percent. Amibo et al. [14] for the study of teff straw, the result was 6.98 percent. The volatile matter obtained for this study was 68.33 percent for wet-based coffee husks. Still, the volatile matter content for dry-based coffee husk was 24.62 percent, which

Table 1: Proximate analysis using the American Society for Testing and Materials (ASTM).

St.	Proximate analysis parameter	Standard methods	Reference	Experimental results
1.	Ash content	ASTM D 1102–84	[14]	3.51
2.	Moisture content	ASTM 2867–99	[23, 27]	10.85
3.	Volatile matter content	ASTM D4607-86	[28]	68.33
4.	Fixed carbon content	ASTM 2867–99	[29]	17.31

Table 2: Proximate analysis performed for different biomass for AC preparation.

Proximate analysis of different biomass for AC preparation	Ash content (%)	Volatile matter (%)	Moisture content (%)	Fixed carbon content (%)	Reference
Coffee husk dry basis	2.01	24.62	6.03	67.34	[30].
Wet basis coffee husk	1–4%	65–72%	10–11%	17–20%	[31]
Wet basis coffee husk	3.51	68.33	10.85	17.31	Current study
Rise husk on a dry basis	21–32%	68–79%	6.0 to 7.7%	19–24%	[29]
Teff straw husk	4.88%	73.61%	6.98%	14.53%.	[14]
Durian shell	2.52	69.59	5.53	22.36	[32]

was supported by previous studies by Ahmad and Rahman [30].

According to Menya et al. [29], the volatile matter content of rice husk ranged between 68 and 79 percent. This result is highly similar to the current study findings. The ash content for this study was 3.51 percent, which is comparable to the previous study finding reported by Amibo et al. [14]. The ash content of the teff straw husk in this study was 4.88 percent. There are a few differences between the outcomes. As shown in Table 2, assessing the proximate analysis aids in determining the ash content of the coffee husk, which aids in determining the capacity of the coffee husk as an alternate source for the synthesis of activated carbon.

This was due to the type of raw material used for activated carbon preparation, the soil they grew in, the environment they were exposed to, and the type of coffee husk used for the experiments. All proximate analysis results and standard methods used were summarized, as shown in Table 1. As a result, the proximate analysis for dry and wet coffee husks yielded different results in terms of ash content, volatile matter content, and moisture content, as shown in Table 2.

3.2. CHAC Physiochemical Properties. Table 3 depicts the physiochemical properties of CHBAC. The experiments yielded the following parameter results: pH, porosity, the yield of CHBAC, bulk density, point of zero charges, and specific surface area. The pH, porosity, yield of CHBAC, bulk density, point of zero charges, and specific surface area obtained during experimentation were 5.2, 58.4 percent, 60.1 percent, 0.71 g/mL, 4.19, and 1396 m^2/g, respectively. According to Amibo et al. [14], the results for teff straw pH, bulk density, point of zero charges, and surface area were 10.8, 0.42 g/mL, and 4.3, respectively. The bulk density and point of zero charges for both coffee husk and teff straw were comparable. Still, the high difference in pH occurred because the coffee husk was impregnated before the ashing process for more activation but not the teff straw. The specific surface

Table 3: Physiochemical properties of CHAC.

St.	Physiochemical properties	CHBAC values obtained
1	Bulk density (g/mL)	0.71
2	pH	5.2
3	pH_{PZC}	4.19
4	Specific surface area (m^2/g)	1396
5	Porosity (%)	58.4
6	The yield of CHAC (%)	60.1

area of coffee husk in a previous study reported by Thi et al. [33], was 1383 m^2/g, which was comparable to the current study finding of 1396 m^2/g.

As shown in Figure 1, the point of zero charge determination for coffee husk-based activated carbon activated by sulfuric acid (H_2SO_4) was 4.19, which was consistent with previous study reports. H-type activated carbons have a positive charge in water, are hydrophobic, and absorb strong acids. L-type activated carbons have a negative charge in water, are hydrophilic, and neutralize strong bases. There has been a lot written on the oxidation of activated carbon [34]. The surface charge of activated carbons 32 is affected by the pH of the solution. When the pH of the solution is less than pH pzc, the carbon surface has a positive surface charge, and when the pH is more than pH pzc, the carbon surface has a negative charge [35]. Therefore, the activated carbon prepared under this study exhibit a positive surface charge and attracts negatively charged $HCrO4^-$. Cr (VI) is attracted to the positively charged carbon surface, reduced to Cr (III) by phenol groups, and adsorbed inside the pores [36].

3.3. Characterization of CHBAC. FTIR and XRD were used to characterize activated carbon produced from the coffee husk. FTIR analysis was used for functional group analysis in this study, with peaks available in the 400 to 4500 cm^{-1} range. Wavenumber and transmittance were used to identify the peaks found in coffee husk when FTIR equipment was used to analyze it. The crystalline index of activated carbon

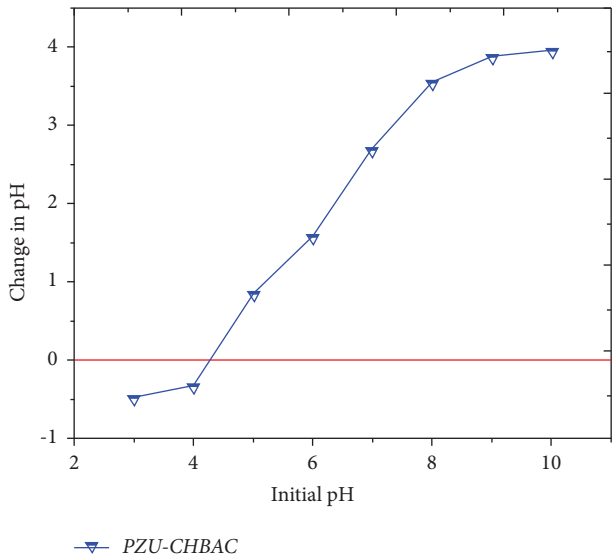

Figure 1: Point of zero charge determination for CHBAC.

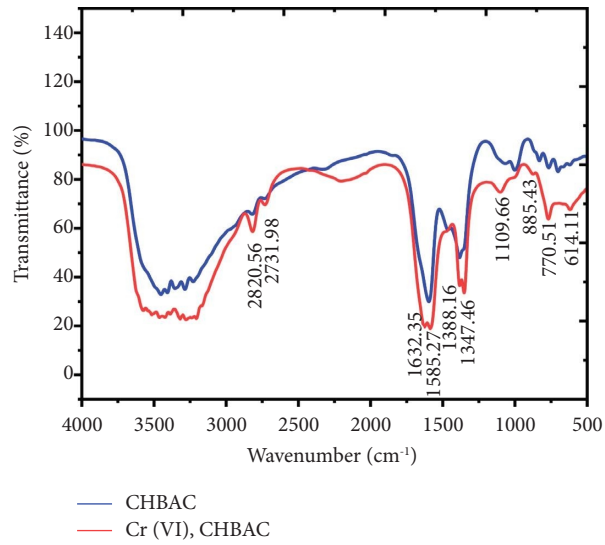

Figure 2: FTIR image for CHBAC and Cr (VI) absorbed on CHBAC.

produced from coffee husk was determined using XRD analysis.

3.3.1. FTIR Analysis. FTIR analysis for coffee husk-based activated carbon, as shown in Figure 2, revealed several peaks, the broad peak available at 3457 cm^{-1} representing the functional group stretch for free and bond hydroxyl (O-H). The bond stretches available on 2942, 1653, 1559, 1378, and 1014 cm^{-1} represent the bond stretches for –CH2, C–C, C=C, C–O, and C–N, respectively, and are consistent with the previous FTIR analysis report of Ayalew and Aragaw, [37]. The bond stretch for N=O, C–N, C=O, and C–S is attributed to around 1645, 1378, 1180, and 670 cm^{-1}, respectively. Such free and double bonds enhance the adsorption capacity of coffee husk-activated carbon. The high specific surface and porosity of coffee husk-activated carbon resulted from the presence of free electrons within the CHBAC. Figure 2 shows that chromium-adsorbed activated carbons had various peaks that were read after adsorption. Beyan et al. [23], back up this work the peak intensities of 1585.27, 1347.46, 770.51, and 614.11 cm^{-1} were available.

3.3.2. XRD Analysis. Figure 3 shows an XRD analysis for CHBAC, which aids in determining the crystalline index and peaks for the produced activated carbon. The peaks available for CHBAC at 2 are 29.9°, 34.08°, 35.8°, 36.9°, 44.77°, 46.23°, 57.87°, and 64.36°. The XRD patterns of activated carbon produced from the coffee husk and nonporous activated carbon produced from the rice husk were similar. According to Xu et al. [38], activated carbon synthesized from rice husks produced XRD patterns that were similar to the current study.

3.4. The Initial and Final Concentration of Cr (VI). According to the study presented by Mustapha et al. [39], most chemicals used in tannery factories included lime,

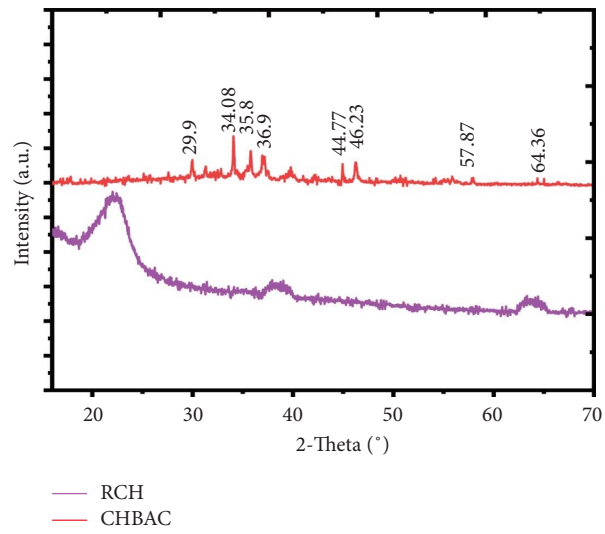

Figure 3: XRD image of coffee husk-based activated carbon (CHBAC).

sodium chloride, sodium bicarbonates, sulfuric acid, chromium sulfate, ammonium sulfate, and heavy metals such as chromium, which existed in the forms Cr(III) and Cr(VI). Because Cr (VI) is more toxic than Cr (III), many researchers are focusing on its removal (VI). As a result, a UV-spectrophotometer was used to determine the initial concentration of Cr (VI). The blank solution was made by excluding Cr (VI) from the previously listed chemicals and compounds. This absorbance was then compared to an aqueous solution prepared on a laboratory scale to determine the concentration of Cr (VI) in tannery wastewater. According to a study conducted by Neelam, [40], the maximum amount of Cr (VI) released from tannery wastewater must be 0.1 mg/L is acceptable. In contrast, the concentration of Cr (VI) in drinking water must be less than 0.05 mg/L [41]. The tanner wastewater concentrations

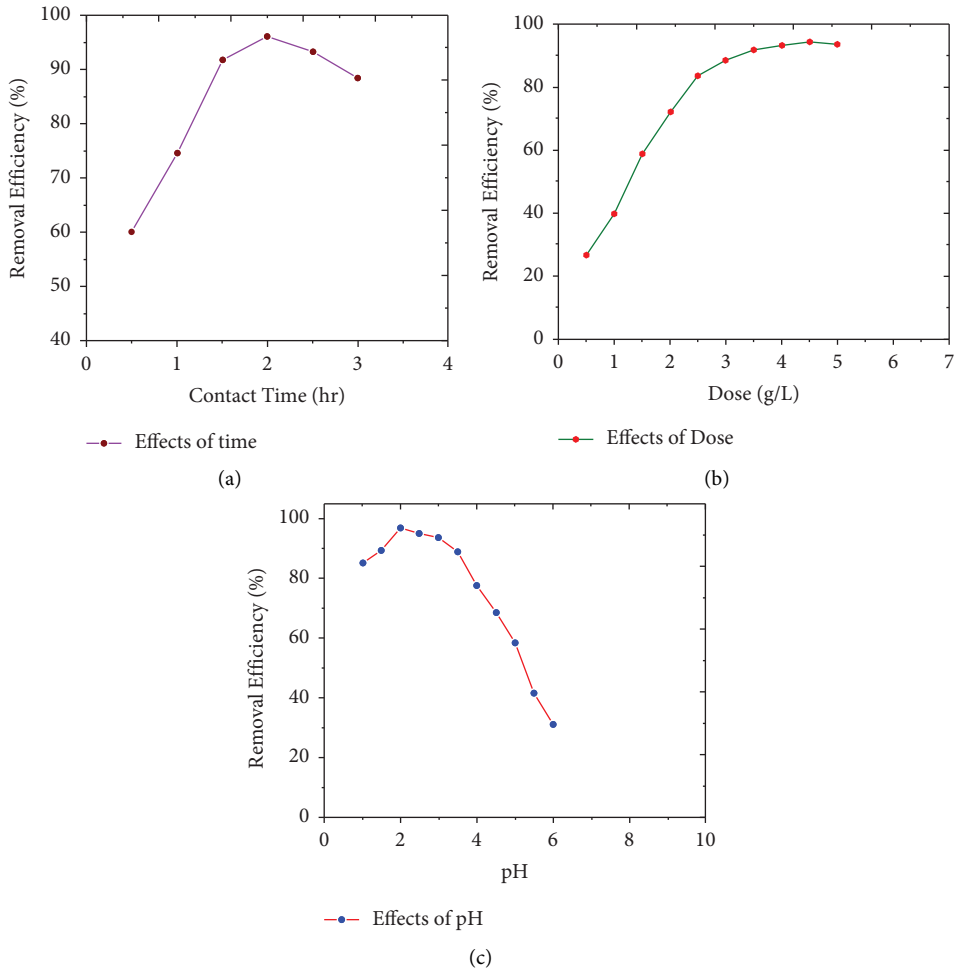

Figure 4: The effects of (a) pH, (b) dose (g/L), and (c) contact time on Cr (VI) removal efficiency.

ranged from 0.12 mg/L to 345 mg/L, violating the standards. In this study, the Cr (VI) concentration directly after treatments was 76 ppm, but after treatment in tannery wastewater, the concentration released into the environment was around 1 ppm.

3.5. The Effects of Individual Factors on Hexavalent Chromium Removal. The adsorption of hexavalent chromium is affected by various factors, including adsorbent dosage, initial concentration, pH, rotational speed, and adsorbent type [42]. The main factors chosen for this study were CHBAC dosage, pH, and contact time, but other factors such as rotational speed and initial concentration were kept constant at 350 rpm and 76 gm/L.

3.5.1. The Effects of pH on Cr (VI) Adsorption. As shown in Figure 2(a), the effects of pH on Cr (VI) adsorption, the adsorption capacity of CHBAC decreased as the pH increased. At lower pH, the adsorption capacity of CHBAC was high due to the low concentration of hydroxyl group present in the solution, as well as the increased positive charge found in activated carbon [23, 43]. Such positive charge increments increase the electrostatic force for the removal of chromate ions found in the solution, such as chromate (CrO_4^{2-}), dichromate ($Cr_2O_7^{2-}$), and acid chromate ($HCrO_4^-$) [42, 44–46]. The maximum adsorption capacity was measured at a pH of 2 in this study, which was supported by a previous study reported by [42]. Most companies, such as tanneries, chromium plating, and electroplating, use wastewater effluents with a pH of around 2, allowing maximum adsorption of Cr (VI).

3.5.2. The Effects of Dose on Cr (VI) Adsorption. As shown in Figure 4(b), as the dose of CHBAC was increased, the adsorption of Cr (VI) increased, which resulted from the presence of vacant active site increments due to adsorbent increases. This study was supported by Gnanasundaram et al. [47]. However, as the adsorbent dose increased above 3 and 4 g/L, the adsorption capacity decreased due to aggregation and instauration on the active site caused by the high concentration of CHBAC [45].

3.5.3. The Effects of Dose on Cr (VI) Adsorption. Contact time is one aspect that influences the adsorption process of Cr (VI) removal from tannery wastewater. As demonstrated in Figure 4(c), as contact time rose, the adsorption process

Table 4: central composite design (CCD) matrix for experimentation.

Run	pH	Dose (g/L)	Contact time (hr.)	Actual Cr (VI) adsorption	Predicted Cr (VI) adsorption
1	3	3	1	74.77	74.99
2	0.3	4	2	79.98	80.05
3	3.7	4	2	78.04	77.89
4	2	4	2	96.99	97.23
5	2	4	2	97.06	97.23
6	2	4	2	97.16	97.23
7	2	4	0.3	72.51	72.35
8	2	4	2	97.36	97.23
9	2	2.3	2	82.95	82.81
10	1	5	1	81.85	81.89
11	2	5.7	2	90.31	90.37
12	3	3	3	79.55	79.57
13	2	4	3.7	78.05	78.13
14	1	3	1	76.81	76.84
15	1	3	3	78.15	78.17
16	2	4	2	97.33	97.23
17	2	4	2	97.46	97.23
18	1	5	3	84.26	84.11
19	3	5	3	83.40	83.43
20	3	5	1	77.91	77.95

Table 5: Effects of individual factors and interaction effects on adsorption of Cr (VI).

Source	Sum of square	Df.	Mean square	F-value	p value	
Model	1518.60	9	168.73	5077.33	<0.0001	Significant
A-pH	5.54	1	5.54	166.73	<0.0001	
B-dose	68.18	1	68.18	2051.65	<0.0001	
C-contact time	39.87	1	39.87	1199.57	<0.0001	
AB	2.16	1	2.16	65.09	<0.0001	
AC	5.31	1	5.31	159.90	<0.0001	
BC	0.3961	1	0.3961	11.92	0.0062	
A^2	594.25	1	594.25	17881.53	<0.0001	
B^2	201.78	1	201.78	6071.79	<0.0001	
C^2	861.81	1	861.81	25932.63	<0.0001	
Residual	0.3323	10	0.0332			
Lack of fit	0.1612	5	0.0322	0.9419	0.5254	Not significant
Pure error	0.1711	5	0.0342			
Cor total	1518.93	19				

increased, and as time extended beyond 2 hours, the adsorption process reduced. At 2 hours, the maximal adsorption process was attained. The adsorption process increased at first, then decreased as the contact duration rose due to an excess of active sites on the adsorbent and, eventually, repulsion between adsorbent ions on the CHBAC and solution ions when time exceeded maximum points [48]. The processes of Cr (VI) adsorption on activated carbon (AC) was investigated and predicted. Adsorption happened in two phases, pore and surface diffusion models. A thin Cr_2O_3 (s) coating covered the AC surface quickly, reducing the adsorption rate due to this reason when the time increased by more than two hours the desorption process was carried out.

3.6. Optimization of Cr (VI) Removal and Central Composite Design. Design expert (V.11.00) software was used to optimize Cr (VI) adsorption. The three factors in this investigation were pH, dosage, and contact time, which varied from 0.3–3.7, 2.3–5.7 g/L, and 0.3–3.7 hr., respectively.

As indicated in Table 4, CCD creates 20 data points for testing, and the design expert matrix for the adsorption capacity of CHBAC on the removal of Cr (VI) varied from 72.51 to 97.46 percent. As shown in Table 5, all independent variables such as pH, dosage, and contact duration had p values less than 0.0001, indicating that they significantly influenced Cr (VI) adsorption capacity. The factors had significant effects on the dependent variable with p values less than 0.05 [49]. The other interaction and self-interaction impacts on adsorption capacity were significant since the p value was less than 0.05. The measured F-Value from the model is 5077.33, indicating its importance, and it has a 0.01 probability of being big owing to noise.

In this scenario, A, B, C, AB, AC, BC, A^2, B^2, and C^2 are significant model terms, whereas the lack of fit model is negligible compared to relative error, with a p value

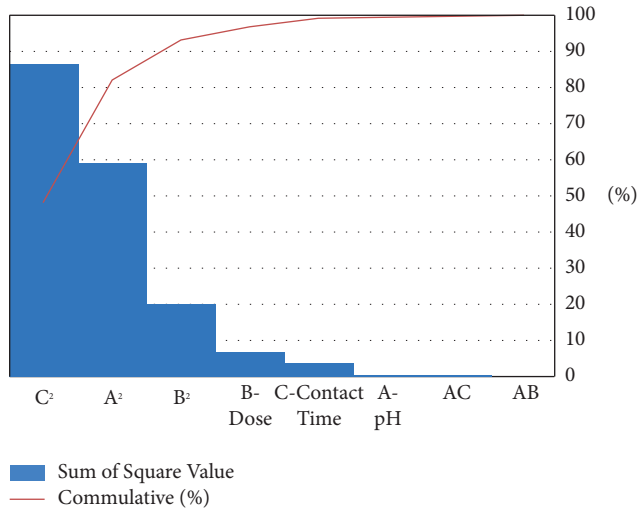

Figure 5: The effects of factors and their interaction effects on response.

larger than 0.05. The factors with the highest sum of squares and F-values have a high significance level on the dependent variable or response [50]. As a result of the larger sum of square and F-value values of 68.18 and 2051.65, respectively, the dose had a greater influence on Cr (VI) adsorption capacity than other factors such as pH and contact duration.

The effects of each component and their interactions were depicted on a Pareto diagram in Figure 5. The major factor was dosage, which had a considerable impact, followed by contact duration and pH of the solution. AC had a considerable influence on the interaction effects, followed by AB. Finally, the self-interaction effects of C2, A2, and B2 influenced the reaction significantly.

3.7. Fit Summary and Statistic. Table 6 summarizes the data for the indicated model, which in this case was the quadratic model. The quadratic model was chosen after examining four models: linear, two factors interacting (2FI), quadratic, and cubic. This was owing to the quadratic model's having a lack of fit. The model was 0.5254, the *p*value was less than 0.0001, the adjusted R^2 was 0.9996, and the anticipated R^2 was 0.9990. The recommended model was chosen based on *p* values, lack of fit, adjusted R^2, and predicted R^2 value. Choose the highest-order polynomial in which the extra terms are important, and the model is not aliased; hence, the cubic model is not chosen since it is aliased [51–54].

Standard deviation (Std. Dev.), mean, coefficients of variation (C.V.), R^2, adjusted R^2, projected R^2, and Adeq Precision were 0.1823, 85.09, 0.2142, 0.9998, 0.9996, 0.9990, and 193.0294, respectively, according to Table 7. According to earlier research, the anticipated and adjusted R^2 were in good agreement, with a difference of less than 0.2 [55–60].

According to equation (3), the variables have an impact on the adsorption capacity both positively and negatively. According to the model equation developed for Cr (VI) adsorption using CCD, dose and contact time had positive effects. As time and dose increased, so did the adsorption capacity, up to a certain limit. The opposite is true for pH, as the pH of the solution increased, the adsorption capacity of Cr (VI) decreased and vice versa. Increasing the pH causes a decrease in adsorption, increasing the dosage causes an increase in adsorption capacity, and increasing the contact duration causes an increase in adsorption capacity for Cr (VI) [61].

$$Cr\,(VI)\text{adsorption} = 97.23 - 0.6341A + 2.22B + 1.70C - 0.5200\text{AB} + 0.8150\text{AC} + 0.2225\text{BC-}6.32A^2 - 3,68B^2 - 7.61C^2, \quad (3)$$

where A represents pH, B stands for dosage, and C stands for contact duration, and the interaction effects are AB, AC, BC, A^2, B^2, and C^2

Figure 6 depicts the actual and expected values for Cr (VI) adsorption, which were created using a CCD matrix based on the actual and predicted values from Table 4. The predicted values were represented by a straight line 45o inclined from the origin, while the actual point was depicted along a line of predicted values; they agreed well, and the R^2 value was 0.9998. The model is more acceptable when the R^2 value approaches one [62–65].

3.8. Optimization of Cr (VI) Adsorption. The 3D depiction for optimizing Cr (VI) adsorption employing three parameters such as dosage (g/L), contact duration (hr.), and pH is illustrated in Figures 7(a), 7(b), and 7(c). The optimal Cr (VI) adsorption by CHBAC was 97.46 percent at a dosage

Table 6: Fit summary for model selection.

Source	Sequential p-value	Lack of fit p-value	Adjusted R^2	Predicted R^2	
Linear	0.7336	<0.0001	−0.0987	−0.2781	
2FI	0.9946	<0.0001	−0.0987	−1.2223	
Quadratic	<0.0001	0.5254	0.9996	0.9990	Suggested
Cubic	0.4253	0.4949	0.9996	0.9996	Aliased

Table 7: Fit statistic fitting and the coefficient of determination (R^2) of data points.

Std. dev.	Mean	C.V. %	R^2	Adjusted R^2	Predicted R^2	Adeq. precision
0.1823	85.09	0.2142	0.9998	0.9996	0.9990	193.0294

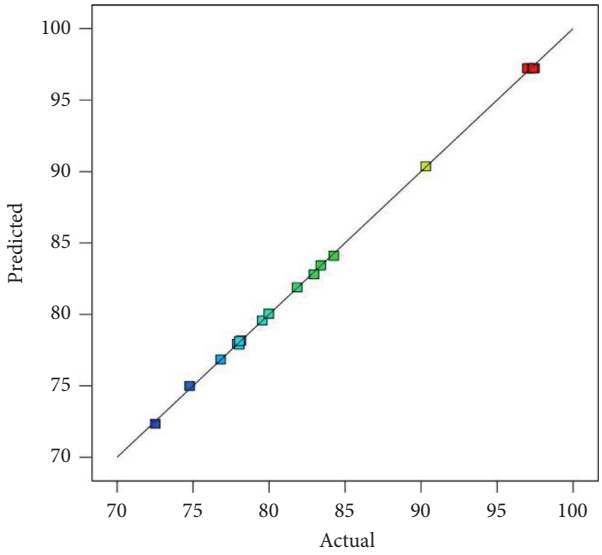

Figure 6: Actual and predicted values for Cr (VI) adsorption.

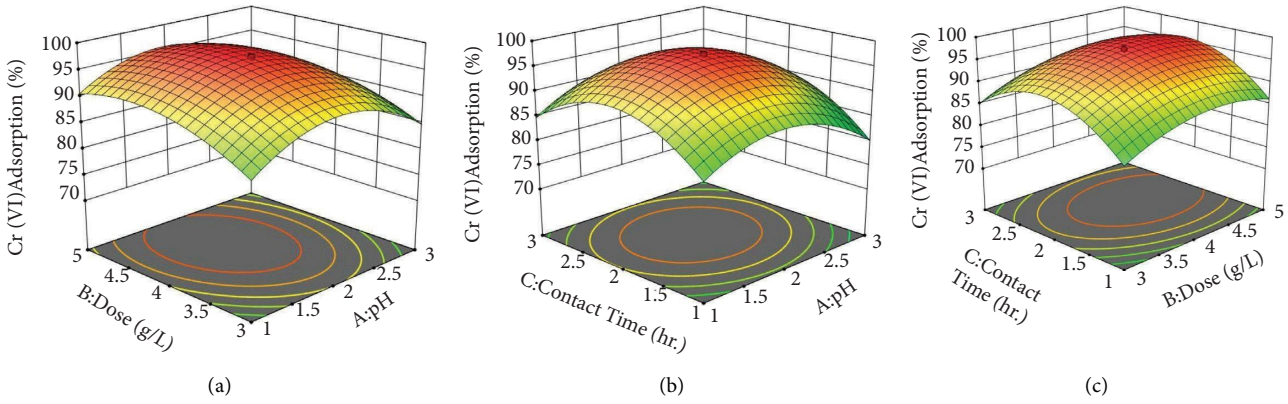

(a) (b) (c)

Figure 7: 3D image for Cr (VI) adsorption, (a) dose (g/L) vs. pH, (b) contact time (hr.) vs. pH, (c) contact time (hr.) vs. dose (g/L).

of 4 g/L, pH of 2, and contact period of 2 hr which was determined from the CCD matrix as shown in Table 4. This improvement resulted in good agreement with the individual impacts indicated in Figures 4(a), 4(b), and 4(c).

The counter line diagrams Figure 8(a), 8(b), and 8(c) had comparable values to the 3D diagram values evaluated. Dots around the center show the best adsorptions. The best results were 97.46 percent. This was achieved using a dosage of 4 g/L, a pH of 2, and a contact duration of 2 hours. The circle with oval forms indicates the same hexavalent chromium adsorption efficiency achieved by utilizing coffee husk-based activated carbon along the line.

3.9. Numerical Optimization and Validation. According to Table 8, the numerical optimization findings for Cr (VI)

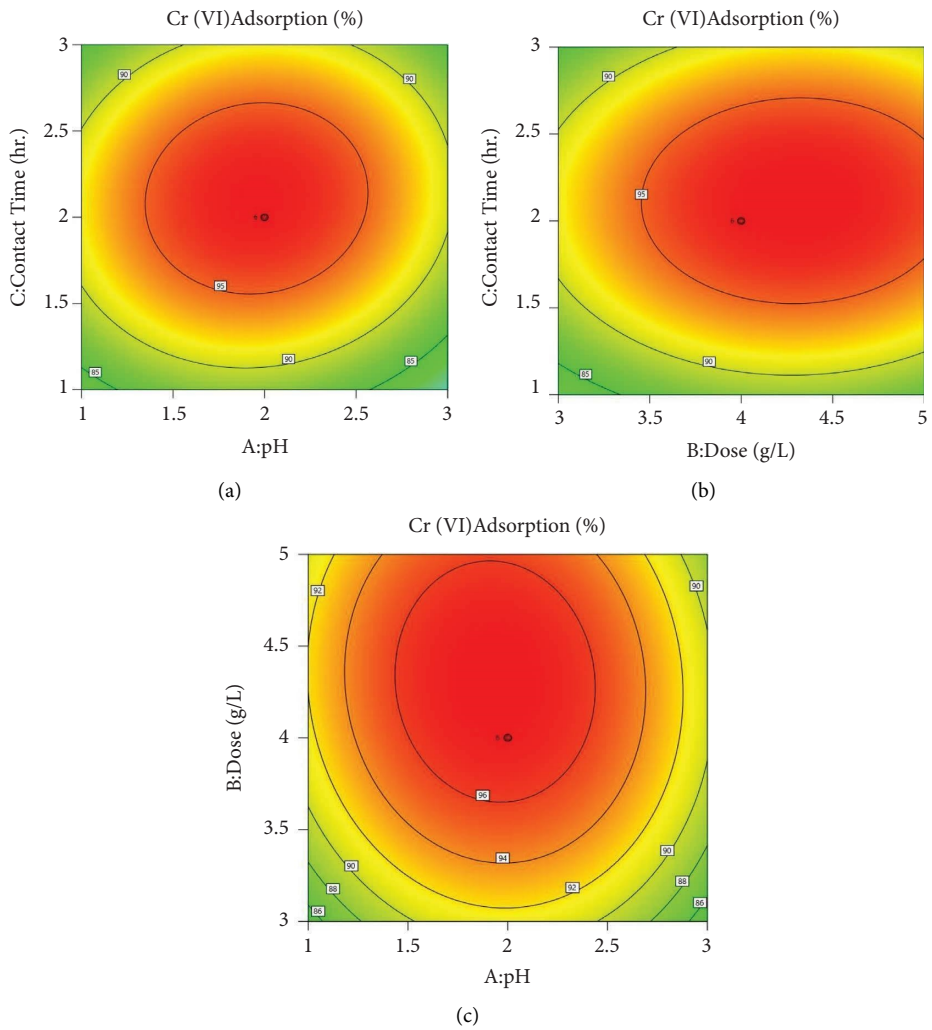

Figure 8: Counter line image for Cr (VI) adsorption, (a) dose (g/L) vs. pH, (b) contact time (hr.) vs. pH, (c) contact time (hr.) vs. dose (g/L).

Table 8: Summary of numerical optimization.

Parameter	Goal	Lower limit	Upper limit	Importance	Optimized values	Desirability
A: pH	Is in range	1	3	3	1.926	1
B: dose	Is in range	3	5	3	4.209	1
C: contact time	Is in range	1	3	3	2.101	1
Cr (VI) adsorption	Maximize	72.51	97.46	5	97.645	1

adsorption were 97.65%. This was achieved at a pH of 1.926, a dosage of 4.209 g/L, and a contact time of 2.101 hr. To validate this numerical optimization, three replication experiments were performed at pH 1.93, a dose of 4.2 g/L, and a contact time of 2.1 hours. The results obtained from the experiments were 97.39 percent, 97.53 percent, and 97.48 percent, with an average value of 97.46 percent, indicating excellent agreement with numerically optimized results. As shown in Figure 9, the desirability for all factors, adsorption efficiency, and combined effects are one.

3.10. Operational Cost to Treat Wastewater. The raw material coffee husk is trash and incurs no expenses. However, to manufacture activated carbon, it incurs expenditures for pretreatment and impregnation by using sodium hydroxide and sulfuric acid. According to Table 9, the operating expenses to treat 1 L of tannery wastewater are 86.545 ETB, which is equivalent to 1.6837 US dollars. This was performed in ten batch experiments to determine the average cost of each experiment. This overall price is high since the experiment was conducted in a laboratory, but the total price

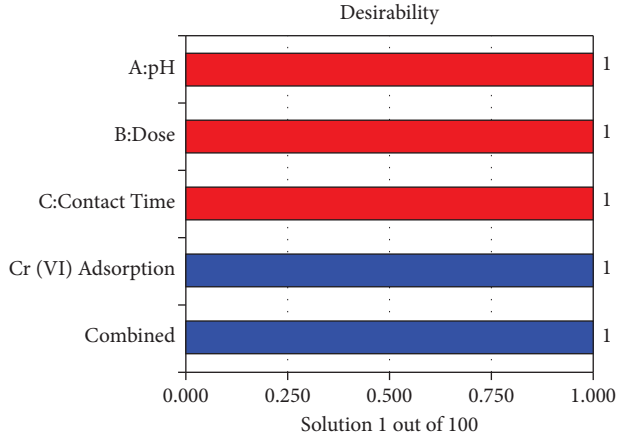

Figure 9: Desirability of factors, adsorption, and combined.

Table 9: Operational costs to treat 1000 mL solution by using 2 g adsorbent.

Raw Material Used				
	Dose (g)	Cost (ETB)	Rate (ETB to $ US)	Cost ($)
Coffee husk	10	7	0.01945	0.1362
Chemicals used				
	Volume (mL)	Cost (ETB)	Rate (ETB to $ US)	Cost ($)
Sulfuric acid	100 (98.3%)	61.476	0.01945	1.196
HCl	100 (38%)	10.28	0.01945	0.2
Mass (g)				
K2Cr2O7	5 (power)	0.771	0.01945	0.015
NaOH	10 (solid pellet)	6.01	0.01945	0.117
Power consumption				
	KW.hr			
During stringing	0.1	1		0.0195
Total cost		86.545		1.6837

Table 10: Comparison of adsorption capacities of Cr(VI) on different adsorbents.

Adsorbent	Adsorption capacity (mg/g)	Adsorption efficiency (%)	Reference
CHBAC	35.82	97.65	Present work
TSCA	19.48	95.90	[23]
ACAP	18.78	96.9	[66]
RSS	15.47	97.80	[67]
ATSAC	21.75	98.00	[68]
PSAC	16.26	95.7	[69]

of the operation is low because all chemicals and other supplies were obtained in bulk.

3.11. Comparison of Adsorption Capacity Biomass-Based Activated Carbon. Based on equation (4) the adsorption capacity was determined and adsorption efficiencies were determined from optimization. The term adsorption capacity refers to how much adsorbate may stick to per gram of adsorbent material. The adsorption capacity of various activated carbons generated from CHBAC, TSCA, ACAP, RSS, ATSAC, and PSAC was 35.82, 19.48, 18.78, 15.47, 21.75, and 16.26, respectively, as shown in Table 10. When compared to earlier findings, it was shown that activated carbon made from coffee husk had a higher adsorption capacity than the other. Therefore, 1 g of activated carbon prepared from coffee husk adsorbs 35.8 mg hexavalent chromium concentration (adsorbent).

$$Q_e = \left(C_O - C_e\right) \times \frac{V}{m}, \tag{4}$$

where Q_e stands for adsorption capacity or equilibrium concentration in mg/g, C_o stands for initial concentration in mg/L, C_i stands for equilibrium concentration in mg/L, V stands for volume of solution in L, and mass of adsorbent taken by g.

4. Conclusion

In this study, biomass-based activated carbon was employed for wastewater treatment. The major three factors investigated were dosage (g), time (hr), and pH. As a result,

CHBAC (coffee husk-based activated carbon) has a high capacity for removing Cr (VI) from tannery effluent. Because of their enormous specific surface area, CHBACs can adsorb a wide range of industrial influents during the adsorption process. FTIR study, XRD analysis, and point zero charges were determined for characterization purposes, indicating that the CHBAC had a good grade of adsorbing ability. A quadratic model has been proposed for Cr (VI) adsorption in this optimization. The *p*values for all independent variables and interaction effects that impact the adsorption process was significant. Both adsorbent dosage and contact duration positively correlated with Cr (VI) adsorption, but pH had the opposite effect. The optimal adsorption of Cr (VI) determined by numerical optimization was 97.46 percent at a pH of 1.93, a dosage of 4.2 g/L, and a contact duration of 2.1 hours. The numerical optimization resulted in a desirability of 1. The operational cost for one liter of waste water is approximately 86.545 ETB (US $1.6837). In this study, the CHBACs have shown outstanding adsorptive capacity and removal efficiency [47].

Data Availability

The data used to support the findings of this study are included in the article.

Conflicts of Interest

The authors declare that there are no conflicts of interest.

Acknowledgments

The authors would like to thank the Faculty of Materials Science and Engineering, Jimma Institute of Technology, and Jimma University.

References

[1] F. Ghorbani, S. Kamari, S. Zamani, S. Akbari, and M. Salehi, "Optimization and modeling of aqueous Cr(VI) adsorption onto activated carbon prepared from sugar beet bagasse agricultural waste by application of response surface methodology," *Surfaces and Interfaces*, vol. 2020, no. 18, Article ID 100444, 2020.

[2] V. Hoffmann, C. Rodriguez Correa, S. Sachs et al., "Activated carbon from corncobs doped with RuO2 as biobased electrode material," *Electronic Materials*, vol. 2, no. 3, pp. 324–343, 2021.

[3] A. B. Bayu, T. Abeto Amibo, and S. M. Beyan, "Adsorptive capacity of calcinated hen eggshell blended with silica gel for removal of lead II ions from aqueous media: kinetics and equilibrium studies," *Journal of Environmental and Public Health*, vol. 2022, Article ID 2882546, 1–16 pages, 2022.

[4] S. M. Beyan, S. V. Prabhu, T. T. Sissay, and A. A. Getahun, "Sugarcane bagasse based activated carbon preparation and its adsorption efficacy on removal of BOD and COD from textile effluents: RSM based modeling, optimization and kinetic aspects," *Bioresource Technology Reports*, vol. 14, Article ID 100664, 2021.

[5] R. R. Karri, G. Ravindran, and M. H. Dehghani, "Wastewater—sources, toxicity, and their consequences to human health," in *Soft Computing Techniques in Solid Waste and Wastewater Management*, pp. 3–33, Elsevier, Amsterdam, Netherlands, 2021.

[6] M. H. Dehghani, G. A. Omrani, and R. R. Karri, "Solid waste—sources, toxicity, and their consequences to human health," in *Soft Computing Techniques in Solid Waste and Wastewater Management*, pp. 205–213, Elsevier, Amsterdam, Netherlands, 2021.

[7] S. Mani, P. Chowdhary, and R. N. Bharagava, "Textile wastewater dyes: toxicity profile and treatment approaches," in *Emerging and Eco-Friendly Approaches for Waste Management*, pp. 219–244, Springer, Singapore, 2019.

[8] P. González-García, "Activated carbon from lignocellulosic precursors: a review of the synthesis methods, characterization techniques, and applications," *Renewable and Sustainable Energy Reviews*, vol. 82, pp. 1393–1414, 2018.

[9] E. Gayathiri, P. Prakash, K. Selvam et al., "Plant microbe based remediation approaches in dye removal: a review," *Bioengineered*, vol. 13, no. 3, pp. 7798–7828, 2022.

[10] F. S. A. Khan, N. M. Mubarak, Y. H. Tan et al., "A comprehensive review on magnetic carbon nanotubes and carbon nanotube-based bucky paper for removal of heavy metals and dyes," *Journal of Hazardous Materials*, vol. 413, Article ID 125375, 2021.

[11] S. M. Beyan, T. A. Ambio, V. P. Sundramurthy, C. Gomadurai, and A. A. Getahun, "Adsorption phenomenon for removal of Pb(II) via teff straw based activated carbon prepared by microwave-assisted pyrolysis: process modelling, statistical optimisation, isotherm, kinetics, and thermodynamic studies," *International Journal of Environmental Analytical Chemistry*, vol. 102, pp. 1–22, 2022.

[12] A. Saravanan, P. Senthil Kumar, S. Jeevanantham et al., "Effective water/wastewater treatment methodologies for toxic pollutants removal: processes and applications towards sustainable development," *Chemosphere*, vol. 280, Article ID 130595, 2021.

[13] A. Demirbas, G. Edris, and W. M. Alalayah, "Sludge production from municipal wastewater treatment in sewage treatment plant," *Energy Sources, Part A: Recovery, Utilization, and Environmental Effects*, vol. 39, no. 10, pp. 999–1006, 2017.

[14] T. A. Amibo, S. M. Beyan, and T. M. Damite, "Novel lanthanum doped magnetic teff straw biochar nanocomposite and optimization its efficacy of defluoridation of groundwater using rsm: a case study of hawassa city, Ethiopia," *Advances in Materials Science and Engineering*, vol. 2021, Article ID 9444577, 1–15 pages, 2021.

[15] A. Bayu, A. Abraham Bekele, T. Abeto, and F. Desalegn, "Conversion of degradable municipal solid waste into fuel briquette: case of Jimma city municipal solid waste," *Iranica Journal of Energy and Environment*, vol. 11, no. 2, 2020.

[16] P. Gutwiński, G. Cema, A. Ziembińska-Buczyńska, K. Wyszyńska, and J. Surmacz-Górska, "Long-term effect of heavy metals Cr(III), Zn(II), Cd(II), Cu(II), Ni(II), Pb(II) on the anammox process performance," *Journal of Water Process Engineering*, vol. 39, Article ID 101668, 2021.

[17] S. S. Qureshi, V. Shah, S. Nizamuddin et al., "Microwave-assisted synthesis of carbon nanotubes for the removal of toxic cationic dyes from textile wastewater," *Journal of Molecular Liquids*, vol. 356, Article ID 119045, 2022.

[18] F. S. A. Khan, N. M. Mubarak, Y. H. Tan et al., "Magnetic nanoparticles incorporation into different substrates for dyes and heavy metals removal—a Review," *Environmental Science & Pollution Research*, vol. 27, no. 35, pp. 43526–43541, 2020.

[19] Z. Rahman and V. P. Singh, "The relative impact of toxic heavy metals (THMs) (arsenic (As), cadmium (Cd), chromium (Cr)(VI), mercury (Hg), and lead (Pb)) on the total environment: an overview," *Environmental Monitoring and Assessment*, vol. 191, no. 7, p. 419, 2019.

[20] H. Liang, R. Sun, B. Song, Q. Sun, P. Peng, and D. She, "Preparation of nitrogen-doped porous carbon material by a hydrothermal-activation two-step method and its high-efficiency adsorption of Cr(VI)," *Journal of Hazardous Materials*, vol. 387, Article ID 121987, 2020.

[21] R. R. Karri, J. N. Sahu, and B. C. Meikap, "Improving efficacy of Cr (VI) adsorption process on sustainable adsorbent derived from waste biomass (sugarcane bagasse) with help of ant colony optimization," *Industrial Crops and Products*, vol. 143, Article ID 111927, 2020.

[22] B. T. Sisay, *Coffee Production and Climate Change in Ethiopia*, Springer, Berlin, Germany, 2018.

[23] S. M. Beyan, S. V. Prabhu, T. A. Ambio, and C. Gomadurai, "A statistical modeling and optimization for Cr(VI) adsorption from aqueous media via teff straw-based activated carbon: isotherm, kinetics, and thermodynamic studies," *Adsorption Science and Technology*, vol. 2022, Article ID 7998069, 1–16 pages, 2022.

[24] T. A. Amibo, S. M. Beyan, and T. M. Damite, "Production and optimization of bio-based silica nanoparticle from teff straw (eragrostis tef) using RSM-based modeling, characterization aspects, and adsorption efficacy of methyl orange dye," *Journal of Chemistry*, vol. 2022, Article ID 9770520, 1–15 pages, 2022.

[25] M. Nasiruddin Khan and A. Sarwar, "Determination of points of zero charge of natural and treated adsorbents," *Surface Review and Letters*, vol. 14, no. 03, pp. 461–469, 2007.

[26] S. Latebo, A. Bekele, T. Abeto, and J. Kasule, "Optimization of trans-esterification process and characterization of biodiesel from soapstock using silica sulfuric acid as a heterogeneous solid acid catalyst," *Journal of Engineering Research*, vol. 10, 2021.

[27] T. A. Amibo, S. M. Beyan, M. Mustefa, V. P. Sundramurthy, and A. B. Bayu, "Development of nanocomposite based antimicrobial cotton fabrics impregnated by nano SiO 2 loaded AgNPs derived from eragrostis teff straw," *Materials Research Innovations*, pp. 1–10, 2021.

[28] S. M. Beyan, T. A. Amibo, and V. P. Sundramurthy, "Development of anchote (Coccinia abyssinica) starch-based edible film: response surface modeling and interactive analysis of composition for water vapor permeability," *Journal of Food Measurement and Characterization*, vol. 16, no. 3, pp. 2259–2272, 2022.

[29] E. Menya, P. W. Olupot, H. Storz, M. Lubwama, and Y. Kiros, "Characterization and alkaline pretreatment of rice husk varieties in Uganda for potential utilization as precursors in the production of activated carbon and other value-added products," *Waste Management*, vol. 81, pp. 104–116, Nov. 2018.

[30] M. A. Ahmad and N. K. Rahman, "Equilibrium, kinetics and thermodynamic of Remazol Brilliant Orange 3R dye adsorption on coffee husk-based activated carbon," *Chemical Engineering Journal*, vol. 170, no. 1, pp. 154–161, 2011.

[31] V. Manasa, A. Padmanabhan, and K. A. Anu Appaiah, "Utilization of coffee pulp waste for rapid recovery of pectin and polyphenols for sustainable material recycle," *Waste Management*, vol. 120, pp. 762–771, 2021.

[32] T. C. Chandra, M. M. Mirna, J. Sunarso, Y. Sudaryanto, and S. Ismadji, "Activated carbon from durian shell: preparation and characterization," *Journal of the Taiwan Institute of Chemical Engineers*, vol. 40, no. 4, pp. 457–462, 2009.

[33] T. Thuy Luong Thi, H. S. Ta, and K. Le Van, "Activated carbons from coffee husk: preparation, characterization, and reactive red 195 adsorption," *Journal of Chemical Research*, vol. 45, no. 5–6, pp. 380–394, 2021.

[34] H.-L. Chiang, C. P. Huang, and P. C. Chiang, "The surface characteristics of activated carbon as affected by ozone and alkaline treatment," *Chemosphere*, vol. 47, no. 3, pp. 257–265, 2002.

[35] L. Fijołek, J. Świetlik, and M. Frankowski, "The influence of active carbon contaminants on the ozonation mechanism interpretation," *Scientific Reports*, vol. 11, no. 1, p. 9934, 2021.

[36] Y. Wang, C. Peng, E. Padilla-Ortega, A. Robledo-Cabrera, and A. López-Valdivieso, "Cr(VI) adsorption on activated carbon: mechanisms, Modeling, and limitations in water treatment," *Journal of Environmental Chemical Engineering*, vol. 8, no. 4, Article ID 104031, 2020.

[37] A. A. Ayalew and T. A. Aragaw, "Utilization of treated coffee husk as low-cost bio-sorbent for adsorption of methylene blue," *Adsorption Science and Technology*, vol. 38, no. 5–6, pp. 205–222, 2020.

[38] H. Xu, B. Gao, H. Cao et al., "Nanoporous activated carbon derived from rice husk for high-performance supercapacitor," *Journal of Nanomaterials*, vol. 2014, Article ID 714010, 1–7 pages, 2014.

[39] S. Mustapha, J. O. Tijani, M. M. Ndamitso et al., "The role of kaolin and kaolin/ZnO nano adsorbents in adsorption studies for tannery wastewater treatment," *Scientific Reports*, vol. 10, no. 1, p. 13068, 2020.

[40] A. Neelam, "Determination of chromium in the tannery wastewater, korangi, karachi," *International Journal of Environmental Sciences & Natural Resources*, vol. 15, no. 4, 2018.

[41] R. A. Fallahzadeh, R. Khosravi, B. Dehdashti et al., "Spatial distribution variation and probabilistic risk assessment of exposure to chromium in groundwater supplies; a case study in the east of Iran," *Food and Chemical Toxicology*, vol. 115, pp. 260–266, 2018.

[42] D. Abdissa, T. Abeto, and Y. Mekonnen, "Adsorptive capacity of coffee husk in the removal of chromium (vi) and zink (ii) from tannery effluent: kinetics and equilibrium studies," vol. 5, no. 2, pp. 54–60, 2021.

[43] F. Gorzin and M. Bahri Rasht Abadi, "Adsorption of Cr(VI) from aqueous solution by adsorbent prepared from paper mill sludge: kinetics and thermodynamics studies," *Adsorption Science and Technology*, vol. 36, no. 1–2, pp. 149–169, 2018.

[44] T. Dula, K. Siraj, and S. A. Kitte, "Adsorption of hexavalent chromium from aqueous solution using chemically activated carbon prepared from locally available waste of bamboo (oxytenanthera abyssinica)," *ISRN Environmental Chemistry*, vol. 2014, Article ID 438245, 1–9 pages, 2014.

[45] B. Kakavandi, R. R. Kalantary, M. Farzadkia et al., "Enhanced chromium (VI) removal using activated carbon modified by zero-valent iron and silver bimetallic nanoparticles," *Journal of Environmental Health Science and Engineering*, vol. 12, no. 1, p. 115, 2014.

[46] T. Abeto Amibo, "Modeling and pulping variables optimization of ethanol-alkali pulping and delignification of grevillea robusta in Ethiopia by response surface methodology," *European Journal of Materials Science and Engineering*, vol. 6, no. 1, pp. 34–51, 2021.

[47] N. Gnanasundaram, M. Loganathan, and A. Singh, "Optimization and Performance parameters for adsorption of Cr6+ by microwave-assisted carbon from Sterculia foetida shells,"

IOP Conference Series: Materials Science and Engineering, vol. 206, Article ID 012065, 2017.

[48] A. Azimi, A. Azari, M. Rezakazemi, and M. Ansarpour, "Removal of heavy metals from industrial wastewaters: a review," *ChemBioEng Reviews*, vol. 4, no. 1, pp. 37–59, 2017.

[49] T. A. Amibo and A. B. Bayu, "Calcium carbonate synthesis, optimization and characterization from egg," *Int. J. Mod. Sci. Technol,* vol. 5, no. 7, pp. 182–190, 2020.

[50] S. M. Beyan, T. A. Amibo, S. V. Prabhu, and A. G. Ayalew, "Production of nanocellulose crystal derived from enset fiber using acid hydrolysis coupled with ultrasonication, isolation, statistical modeling, optimization, and characterizations," *Journal of Nanomaterials*, vol. 2021, pp. 1–12, 2021.

[51] A. Dargahi, M. Vosoughi, S. Ahmad Mokhtari, Y. Vaziri, and M. Alighadri, "Electrochemical degradation of 2, 4-Dinitrotoluene (DNT) from aqueous solutions using three-dimensional electrocatalytic reactor (3DER): degradation pathway, evaluation of toxicity and optimization using RSM-CCD," *Arabian Journal of Chemistry*, vol. 15, no. 3, Article ID 103648, 2022.

[52] M. R. Samarghandi, A. Ansari, A. Dargahi et al., "Enhanced electrocatalytic degradation of bisphenol A by graphite/β-PbO2 anode in a three-dimensional electrochemical reactor," *Journal of Environmental Chemical Engineering*, vol. 9, no. 5, Article ID 106072, 2021.

[53] M. R. Samarghandi, A. Dargahi, A. Rahmani, A. Shabanloo, A. Ansari, and D. Nematollahi, "Application of a fluidized three-dimensional electrochemical reactor with Ti/SnO2–Sb/β-PbO2 anode and granular activated carbon particles for degradation and mineralization of 2, 4-dichlorophenol: process optimization and degradation pathway," *Chemosphere*, vol. 279, Article ID 130640, 2021.

[54] A. Dargahi, H. Rahimzadeh Barzoki, M. Vosoughi, and S. Ahmad Mokhtari, "Enhanced electrocatalytic degradation of 2, 4-Dinitrophenol (2, 4-DNP) in three-dimensional sono-electrochemical (3D/SEC) process equipped with Fe/SBA-15 nanocomposite particle electrodes: degradation pathway and application for real wastewater," *Arabian Journal of Chemistry*, vol. 15, no. 5, Article ID 103801, 2022.

[55] A. Dargahi, K. Hasani, S. A. Mokhtari, M. Vosoughi, M. Moradi, and Y. Vaziri, "Highly effective degradation of 2, 4-Dichlorophenoxyacetic acid herbicide in a three-dimensional sono-electro-Fenton (3D/SEF) system using powder activated carbon (PAC)/Fe3O4 as magnetic particle electrode," *Journal of Environmental Chemical Engineering*, vol. 9, no. 5, Article ID 105889, 2021.

[56] R. Shokoohi, A. J. Jafari, A. Dargahi, and Z. Torkshavand, "Study of the efficiency of bio-filter and activated sludge (BF/AS) combined process in phenol removal from aqueous solution: determination of removing model according to response surface methodology (RSM)," *Desalin. WATER Treat,* vol. 77, pp. 256–263, 2017.

[57] S. Afshin, Y. Rashtbari, M. Vosough et al., "Application of Box–Behnken design for optimizing parameters of hexavalent chromium removal from aqueous solutions using Fe3O4 loaded on activated carbon prepared from alga: kinetics and equilibrium study," *Journal of Water Process Engineering*, vol. 42, Article ID 102113, 2021.

[58] S. Alizadeh, H. Sadeghi, M. Vosoughi, A. Dargahi, and S. A. Mokhtari, "Removal of humic acid from aqueous media using Sono-Persulphate process: optimization and modelling with response surface methodology (RSM)," *International Journal of Environmental Analytical Chemistry*, pp. 1–15, 2020.

[59] A. Bekele Bayu, T. Abeto Amibo, and S. M. Beyan, "Process optimization for acid hydrolysis and characterization of bioethanol from leftover injera waste by using response surface methodology: central composite design," *International Journal of Analytical Chemistry*, vol. 2022, Article ID 4809589, 1–10 pages, 2022.

[60] S. Latebo, A. Bekele, T. Abeto, and J. Kasule, "Optimization of Trans-esterification Process and Characterization of Biodiesel from Soapstock Using Silica Sulfuric Acid as a Heterogeneous Solid Acid Catalyst," *Journal of Engineering Research*, vol. 10, no. 1, pp. 78–100, 2022.

[61] K. Hasani, M. Moradi, S. A. Mokhtari, H. Sadeghi, A. Dargahi, and M. Vosoughi, "Degradation of basic violet 16 dye by electro-activated persulfate process from aqueous solutions and toxicity assessment using microorganisms: determination of by-products, reaction kinetic and optimization using Box–Behnken design," *International Journal of Chemical Reactor Engineering*, vol. 19, no. 3, pp. 261–275, 2021.

[62] A. Azizi, A. Dargahi, and A. Almasi, "Biological removal of diazinon in a moving bed biofilm reactor – process optimization with central composite design," *Toxin Reviews*, vol. 40, no. 4, pp. 1242–1252, 2021.

[63] A. Almasi, "Application of response surface methodology on cefixime removal from aqueous solution by ultrasonic/photooxidation," *International Journal of Pharmacy and Technology*, vol. 8, no. 3, pp. 16728–16736, 2016.

[64] M. R. Samarghandi, D. Nemattollahi, G. Asgari, R. Shokoohi, A. Ansari, and A. Dargahi, "Electrochemical process for 2, 4-D herbicide removal from aqueous solutions using stainless steel 316 and graphite Anodes: optimization using response surface methodology," *Separation Science and Technology*, vol. 54, no. 4, pp. 478–493, 2019.

[65] A. Dargahi, M. Mohammadi, F. Amirian, A. Karami, and A. Almasi, "Phenol removal from oil refinery wastewater using anaerobic stabilization pond modeling and process optimization using response surface methodology (RSM)," *Desalin. WATER Treat,* vol. 87, pp. 199–208, 2017.

[66] I. Enniya, L. Rghioui, and A. Jourani, "Adsorption of hexavalent chromium in aqueous solution on activated carbon prepared from apple peels," *Sustainable Chemistry and Pharmacy*, vol. 7, pp. 9–16, 2018.

[67] Ş. Parlayici and E. Pehlivan, "Comparative study of Cr(VI) removal by bio-waste adsorbents: equilibrium, kinetics, and thermodynamic," *J. Anal. Sci. Technol,* vol. 10, no. 1, p. 15, 2019.

[68] D. Mohan, K. P. Singh, and V. K. Singh, "Removal of hexavalent chromium from aqueous solution using low-cost activated carbons derived from agricultural waste materials and activated carbon fabric cloth," *Industrial & Engineering Chemistry Research*, vol. 44, no. 4, pp. 1027–1042, 2005.

[69] Z. A. Al-Othman, R. Ali, and M. Naushad, "Hexavalent chromium removal from aqueous medium by activated carbon prepared from peanut shell: adsorption kinetics, equilibrium, and thermodynamic studies," *Chemical Engineering Journal*, vol. 184, pp. 238–247, 2012.